https://dx.doi.org/10.4314/dujopas.v10i3c.16
ISSN (Print): 2476-8316
ISSN (Online): 2635-3490
Dutse Journal of Pure and Applied Sciences (DUJOPAS), *Vol. 10 No. 3c September 2024*

Upper Convected Maxwell Fluid in an Isothermal Flow with Thermal Radiation

[*1]Sabiki Adebola Idowu; [1]Mustapha Adewale Usman; [2]Benjamin Aina Peter; [3]Akeem Babatunde Sikiru and [4]Sheriffat Taiwo Ayeni

[*1]Department of Mathematical Sciences,
Olabisi Onabanjo University,
Ago-Iwoye,
Nigeria.

[2]Department of Mathematics and Statistics,
Kampala International University,
Kampala,
Uganda.

[3]Department of Physical,
Mathematical and Computer Sciences,
Aletheia University,
Ago-Iwoye,
Nigeria.

[4]Department of General Studies,
Gerar University of Medical Sciences,
Imope-Ijebu,
Nigeria.

Email: sabiq.idowu@ymail.com

Abstract
In this research paper, a mathematical model of the isothermal flow of upper convected Maxwell (UCM) fluid with thermal radiation through a saturated porous media was studied in detail, with different physical parameters being considered. Maple 18 software is used to implement this strategy. The analysis of the results showed that the flow system was significantly influenced by the Schmidt, Darcy, and Deborah numbers, the unsteadiness parameter, the Maxwell parameter, the magnetic field parameter, and other physical characteristics. The influence of several physical characteristics on the flow system are discussed and shown graphically.

Keywords: Upper Convected Maxwell Fluid; Isothermal flow; Thermal Radiation; Porous Medium; Viscosity

INTRODUCTION
The investigations of non-Newtonian fluids in porous media have attracted the attention of numerous scholars in recent times. This is because of its wide range of industrial and engineering applications, which include, to mention a few, oil reservoir engineering, food technology, applied geophysics, geology, groundwater flow, and oil recovery operations. In

Author for Correspondence

engineering, fluid flow analysis is essential. Transport processes in porous media are the subject of numerous technical and biological fields. Abdelsalam *et al*. (2023); Fetecau *et al*. (2021); Gbadeyan & Dada (2013); Peter *et al.* (2019a); Peter *et al.* (2019b) and Uscilowska (2008) are six examples.

Recent advances in technology, the practical importance of non-Newtonian fluids, and the explosive rise of modern industrial materials have made them more popular than Newtonian fluids. Numerous fluids utilized in industrial environments exhibit non-Newtonian characteristics and actions. Moreover, when the activities occur at a high temperature, the effects of radiation are not insignificant. Thermal radiation is an important heat transfer process manager through heat-regulating variables being heated or cooled. Heat transfer and radiation from the exterior of a heated mass submerged in a fluid-saturated porous media have numerous uses in geophysics and engineering. Depending on the material's geometry and surface properties, radiation can have an impact on heat transfer and flow in porous media. As cited in Jhankal and Kumar (2015); Kashyap, Ojjela & Das (2019); Li *et al.* (2010); Marinca *et al.* (2014); Mukhopadiyay (2012) and Vidyasagar *et al.* (2012).

Previous studies and research overlooked the combined effects of heat radiation, magnetic field, viscous dissipation and thermal conductivity. Thus, the combined effects of thermal radiation, viscous dissipation, magnetic field, and thermal conductivity on the isothermal flow of non-Newtonian fluid in a porous media were assessed in this work using the upper convected Maxwell model.

Mathematical Formulation

We considered unsteady, laminar flow of an incompressible fluid through saturated porous media fills the channel, and it is believed that the flow is irregular. The flow is described by the UCM model for explaining shear. The equations take on the following forms according to Vajravelu *et al.(*2017); Mukhopadhya & Gorla (2012) and Ibrahim & Negera (2020):

$$\frac{\partial w}{\partial x}+\frac{\partial z}{\partial y}=0 \tag{1}$$

$$\rho\left[\frac{\partial w}{\partial t}+w\frac{\partial w}{\partial x}+z\frac{\partial w}{\partial y}+\lambda\left(w^2\frac{\partial^2 w}{\partial x^2}+z^2\frac{\partial^2 w}{\partial y^2}+2wz\frac{\partial^2 w}{\partial x\partial y}\right)\right]=\frac{\partial}{\partial y}\left(\mu\frac{\partial w}{\partial y}\right)$$
$$+2\frac{\partial}{\partial y}\left[\beta_2\left(\frac{\partial w}{\partial y}\right)^3\right]+\frac{\alpha_2}{t^a}\frac{\partial^3 w}{\partial t\partial y^2}-\Phi\frac{\mu_{ef}}{K}w\left(1+\lambda\frac{\partial w}{\partial y}\right)-\sigma B_0{}^2 w\left(1+\lambda\frac{\partial w}{\partial y}\right) \tag{2}$$

$$\rho C_P\left[\frac{\partial T}{\partial t}+w\frac{\partial T}{\partial x}+z\frac{\partial T}{\partial y}+\lambda\left(w^2\frac{\partial^2 w}{\partial x^2}+z^2\frac{\partial^2 w}{\partial y^2}+2wz\frac{\partial^2 w}{\partial x\partial y}\right)\right]=\frac{\partial}{\partial y}\left(k\frac{\partial w}{\partial T}\right)-\frac{\partial q_r}{\partial y}$$
$$+\mu\left(\frac{\partial w}{\partial y}\right)^2+\frac{\alpha_2}{t^a}\frac{\partial^3 w}{\partial t\partial y^2}+2\beta_2\left(\frac{\partial w}{\partial y}\right)^4+w^2\frac{\mu_{ef}}{K}+QC_0AYe^{-\frac{E}{RT}}+Q\left(T-T_0\right) \tag{3}$$

Under the following conditions

$$z=0,\quad T=T_0,\quad w=U_w,\quad -k\frac{\partial T}{\partial y}=h_f\left(T_f-T\right)\ \text{at}\ y=0$$
$$w=0,\quad T=T_f\quad \text{as}\ y\to\infty \tag{4}$$

where $w=$ x-direction, $z=$ y-direction, $\rho=$ Fluid density, $\lambda=$ Relaxation time, $\mu=$ Viscosity, β_2 and $\alpha_2=$ Non-Newtonian fluids, $\mu_{ef}=$ Effective viscosity, $B_0{}^2=$ Uniform magnetic field, $C_P=$ Specific heat, $T=$ Fluid temperature, $Q=$ Heat released due to exothermic reaction, $q_r=$ Radiation heat flux, $A=$ Arrhenius pre-exponential factor, $E=$ Activation energy, $T_0=$ Initial fluid temperature, $T_f=$ Ambient temperature and $h_f=$ Heat transfer coefficient.

$$\frac{\partial q_r}{\partial y}=-\frac{16T_\infty{}^3\sigma^r}{3k^r}\frac{\partial}{\partial y}\left(\frac{\partial T}{\partial y}\right) \tag{5}$$

In order to transform equations (2) – (5),

$$w'=\frac{w}{l_0},\quad z'=\frac{z}{l_0},\quad x'=\frac{x}{l_0},\quad t'=\frac{v_0}{l_o}t,\quad \theta(\eta)=\frac{T-T_0}{T_f-T_0},\quad \varepsilon=\frac{RT_0}{E},\quad \eta=\sqrt{\frac{U_w}{xv_0}}y,$$
$$z=-\frac{\partial\psi}{\partial x}=-\sqrt{\frac{av_0}{1-ct}}f(\eta),\quad w=\frac{\partial\psi}{\partial y}=U_w f(\eta),\quad U_w=\frac{ax}{1-ct},\quad U_P=\frac{c}{2(1-ct)},\quad \delta=\frac{U_w{}^2 l_0}{x}\lambda_1,$$
$$\mathrm{Re}=\frac{\rho x v_0{}^2 l_0}{\mu U_w{}^2},\quad \beta_n=\frac{U_w{}^5}{\nu_0{}^3 x^2}\beta_2,\quad \alpha_n=\frac{U_w{}^2}{\rho l_0 v_0 x t^a}\alpha_2,\quad \Lambda=\lambda\sqrt{\frac{U_w{}^3}{xv_0}},\quad M_0=\frac{l_0 U_w}{\rho\nu_0}\sigma B_0{}^2,$$
$$\mathrm{Pr}=\frac{\rho C_P x l_0 v_0{}^2}{kU_w},\qquad Ec=\frac{E\mu l_0 U_w{}^3}{\rho C_P v_0{}^2 x R T_0{}^2},\qquad R_d=\frac{4T_\infty{}^3\sigma^r U_w}{K^r\rho C_P x v_0{}^2 l_0},\qquad Da=\frac{\rho\nu_0}{l_0\mu_{ef}}K,$$
$$\Psi=\frac{El_0 e^{-\frac{E}{RT_0}}}{RT_0{}^2 v_0\rho C_P}QC_0AY,\ Q_1=\frac{l_0 Q}{v_0\rho C_P},\ Bi=\frac{h_f}{k\left(\frac{U_w}{xv_0}\right)^{\frac{1}{2}}}. \tag{6}$$

Where l_o is a reference length scale, v_o is a reference velocity, θ is a dimensionless temperature, η is the similarity variable, $f(\eta)$ is the dimensionless form of velocity, $f'(\eta)$ is the partial differentiation with respect to η, θ is non-dimensional temperature, ψ is the stream function, U_P is the unsteadiness parameter, δ is the Deborah number, Re is the Reynolds number, β_n is a non-Newtonian parameter, α_n is a non-Newtonian parameter, Λ Maxwell parameter, Da is the Darcy number and Pr is the Prandtl number, Ec is the Ecket number, R_d is the radiation parameter, Bi is the Biot number, Ψ is the Frank-Kamenetskii parameter , Q_1 is the heat source parameter

Equations (6), (1) – (5) and dropping the primes yield

$$f''\left(U_p\eta-\eta f'-f\right)+\delta\left\{f'^2\left(\eta^2 f'''+2\eta f''\right)+f^2 f'''+ff'\left(\eta f'''+f''\right)\right\}=\frac{1}{\mathrm{Re}}f'''$$
$$+2\beta_n f''^2 f'''+U_P\alpha_n\left(\eta f''''+f'''\right)-\frac{1}{Da}\Phi_1 f'\left(1+\Lambda f''\right)-M_0{}^2 f'\left(1+\Lambda f''\right) \quad (7)$$

$$\theta'\left(U_P\eta-\eta f'-f\right)+\delta\left\{f'^2\left(\eta^2 f'''+2\eta f''\right)+f^2 f'''+ff'\left(\eta f'''+f''\right)\right\}=\frac{1}{\mathrm{Pr}}\theta''$$
$$+\frac{4}{3}R_d\theta''+Ecf''^2+U_P\alpha_n\left(\eta f''''+f'''\right)+2\beta_n f''^4+\frac{1}{Da}f'^2+\psi e^{\frac{\theta}{1+\varepsilon\theta}}+Q_1\theta \quad (8)$$

The modified boundary conditions, equation (4) are as follows:

$$f(\eta)=0,\ \theta(\eta)=0,\ f'(\eta)=1,\ \theta'(\eta)=-Bi\left(1-\theta\right) \quad \text{at} \quad \eta=0,$$
$$f'(\eta)=0,\quad \theta(\eta)=1,\quad \text{as} \quad \eta\to\infty \quad (9)$$

3 Method of Solution

Galerkin-weighted residual approach is utilized to numerically solve the coupled non-linear governing boundary layer equations (9) and (10) and their corresponding boundary conditions (11) through the use of f solution in the Maple 18 software.

$$\text{Let}\ \ f=\sum_{i=0}^{2}A_i e^{\left(-\frac{i}{5}\right)y},\quad \theta=\sum_{i=0}^{2}B_i e^{\left(-\frac{i}{5}\right)y} \quad (10)$$

We use the following parameter values:

$$U_p=\Lambda=0.1,\delta=0.3,\mathrm{Re}=0.5,\beta_n=M_0=0.4,\alpha_n=0.6,\Lambda=0.1,Da=0.2,Ec=1.5,Q_1=0.45,$$
$$R_d=1.3,Ec=1.5,\psi=1.8,\mathrm{Pr}=1.2 \quad (11)$$

These will be the default values in this work.

RESULTS AND DISCUSSION

Figures 1 through 16 display the results in the following manner: Figures 1–2 depict the effects of the unsteadiness parameter on the temperature and velocity fields. It should go without saying that raising the unsteadiness parameter raises the velocity. As the unsteadiness parameters rise, it looks that the temperature profile is getting lower. Dimensionless patterns of temperature and velocity for a range of Deborah number values are shown in Figures 3–4. As Deborah's number increases, the velocity and temperature profiles seem to be getting smaller. Dimensionless patterns of temperature and velocity for different Darcy numbers are shown in Figures 5–6. As the Darcy number rises, a reduction in the velocity and temperature profiles is seen. The impact of magnetic variables on the velocity profile is seen in Figure 7. It is observed that as the magnetic parameter increases, the velocity profile decreases. The impact of Reynolds number on the velocity field is shown in Figure 8. It goes without saying that the velocity profiles increase as the Reynolds number does.

Figures 9 and 10 illustrate how the radiation parameter and the Prandtl number affect temperature profiles. The temperature profiles decrease as the radiation parameter and Prandtl number increase. The dimensionless temperature curve for various non-Newtonian parameter values is shown in Figure 11. As the non-Newtonian parameters rise, the temperature profile decreases. The impact of the porosity parameter on the velocity field is shown in Figure 12. It is evident that the velocity profile decreases as the porosity parameter increases. Figures 13–14 illustrate how the Ecket number and Frank-Kamenetskii parameter, affect temperature profiles. When Frank-Kamenetskii parameter and Ecket number rise, it is evident that the temperature profiles decrease.

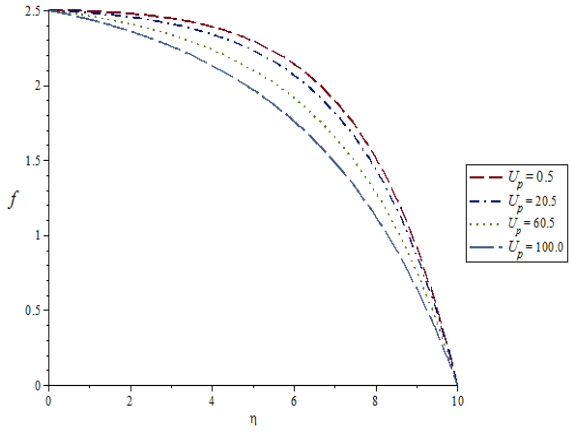

Fig. 1. Impact of U_p on f

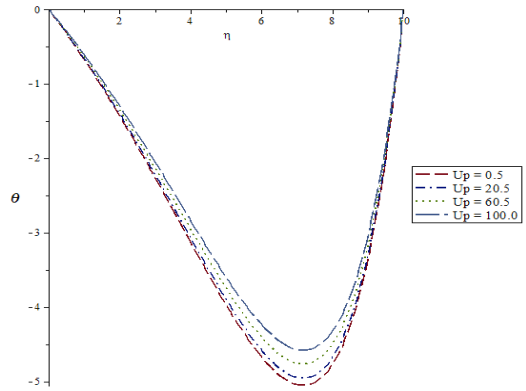

Fig. 2. Impact of U_p on θ

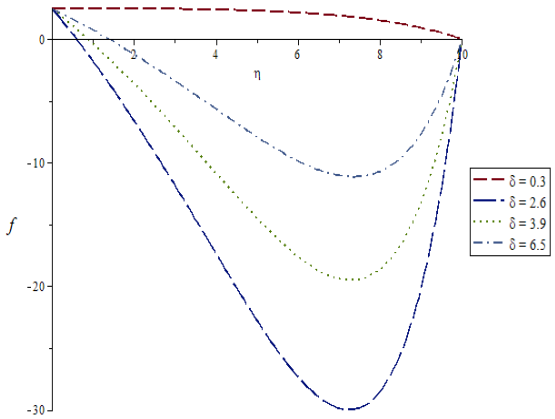

Fig. 3. Impact of δ on f

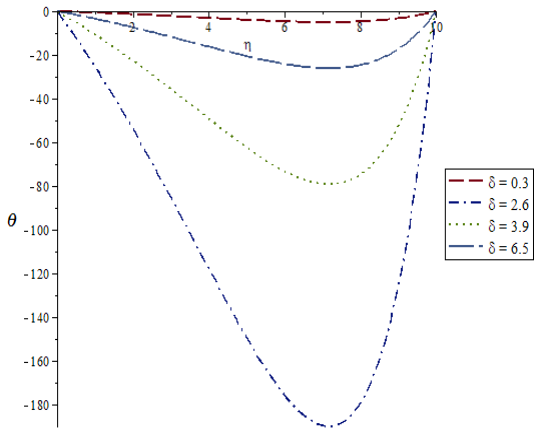

Fig. 4. Impact of δ on θ

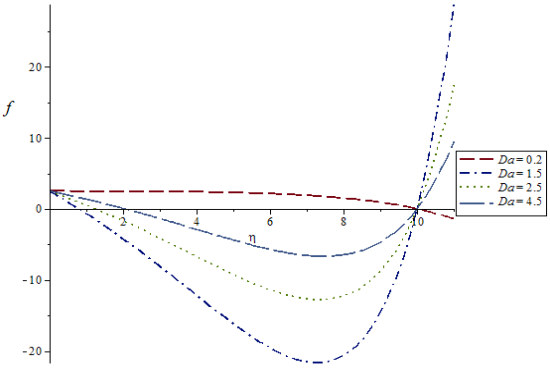

Fig. 5. Impact of Da on f

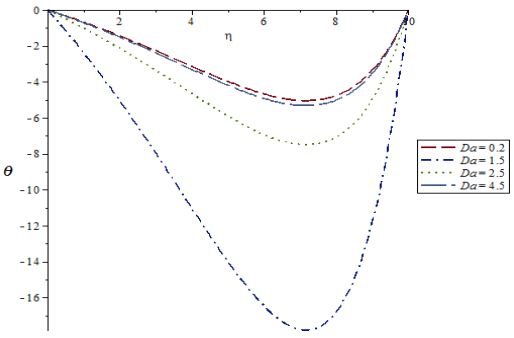

Fig. 6. Impact of Da on θ

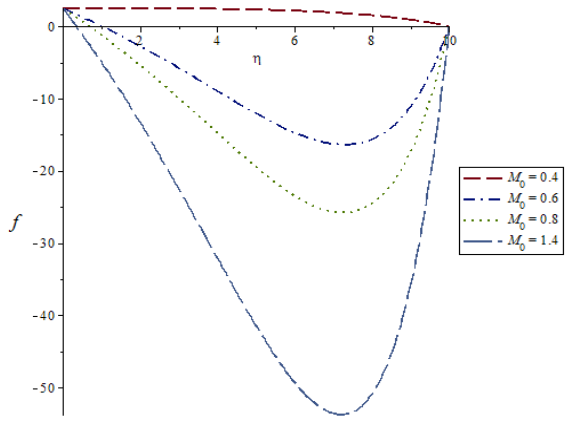

Fig. 7. Impact of M_0 on f

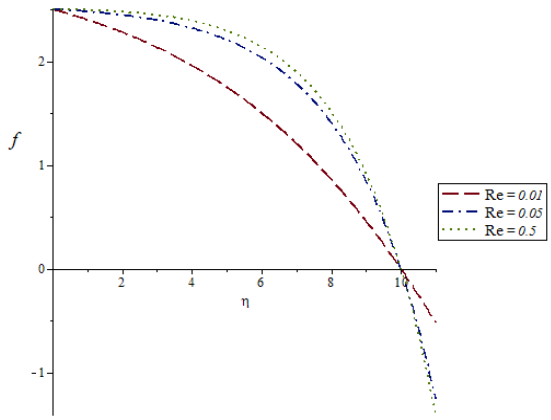

Fig. 8. Impact of Re on f

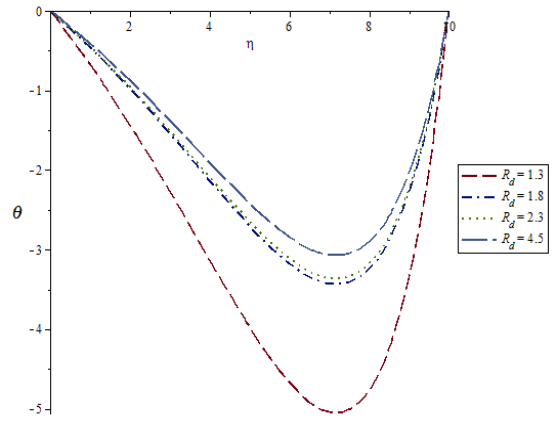

Fig. 9. Impact of R_d on θ

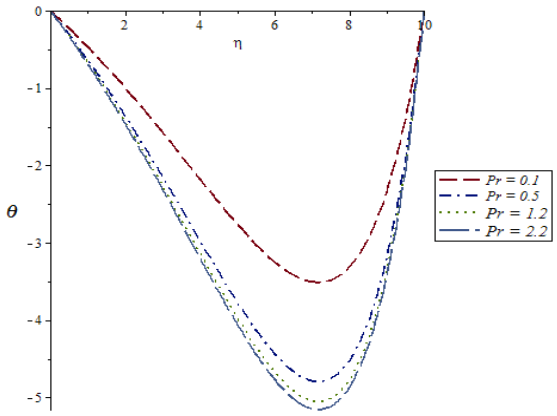

Fig. 10. Impact of Pr on θ

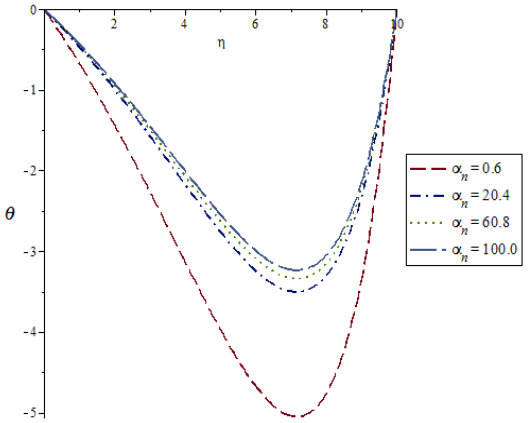

Fig. 11. Impact of α_n on θ

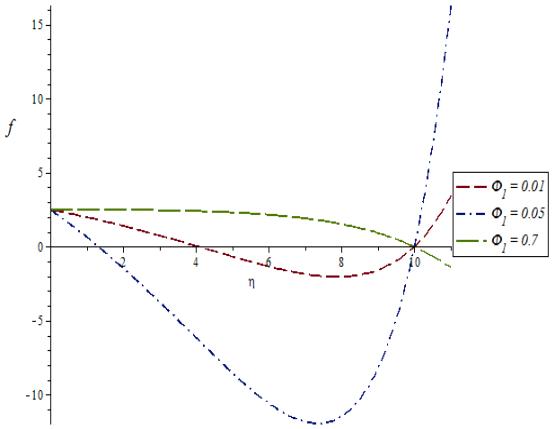

Fig. 12. Impact of Φ_1 on f

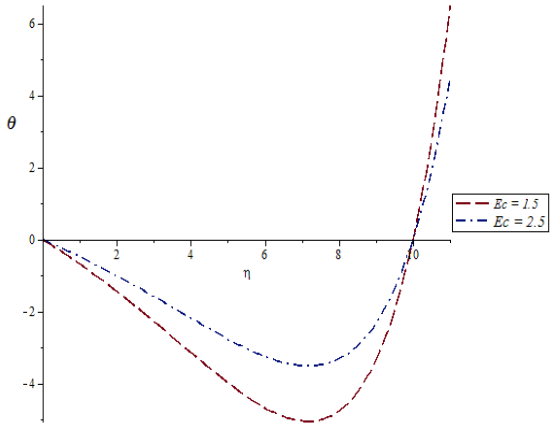

Fig. 13. Impact of Ec on θ

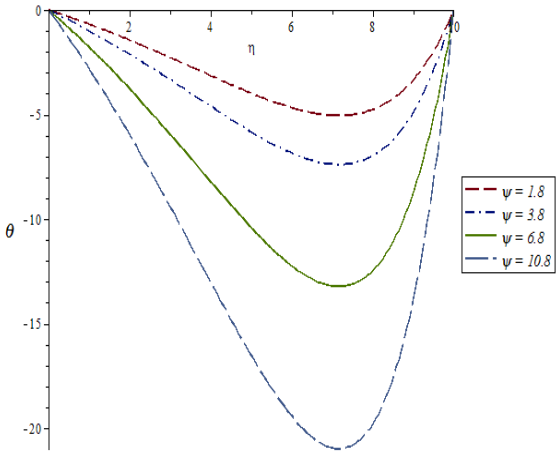

Fig.14. Impact of ψ on θ

CONCLUSION

This work revealed that thermal radiation parameter, variable thermal conductivity and viscosity parameters, magnetic field and third grade fluid parameters, and others have a significant impact on the mass flow and the energy transfer phenomena in the flow system. It was observed that temperature and velocity of the fluids increase when the value of variable viscosity parameter increases.

REFERENCES

Abdelsalam, S.I., Abass, W., Megahed, A.M., and Said, A.A.M. (2023) 'A comparative study on the rheological properties of upper convected Maxwell fluid along a permeable stretched sheet', *Heliyon*, 9(12), pp. 1-13.

Fetecau, C., Vieru, D., Abbas, T. and Ellahi, R. (2021) 'Analytical solutions of upper convected Maxwell fluid with exponential dependence of viscosity under the influence of pressure', *Mathematics*, 9(4), pp. 202-216.

Gbadeyan J.A. and Dada M.S. (2013) 'On the influence of radiation and heat transfer on an unsteady MHD non-Newtonian fluid flow with slip in a porous medium', *Journal of Mathematics Research,* 5(3), pp. 40 – 50.

Ibrahim, W. and Negera, M. (2020) 'MHD slip flow of upper-convected Maxwell nanofluid over a stretching sheet with chemical reaction', *Journal of the Egyptian Mathematical Society*, 28(7), pp. 1-8.

Jhankal, A.K. and Kumar, M. (2015) 'MHD boundary layer flow and heat transfer of an upper-convected Maxwell fluid', *International Journal of Mathematical Archieve,* 6(2), pp. 73-78.

Kashyap, K.P., Ojjela, O. and Das, S.K. (2019) 'Magnetohydrodynamic mixed convective flow of an upper convected Maxwell fluid through variably permeable dilating channel with Soret effect', *Pramana – J. Phys*., 92(73), pp. 1 – 10.

Li, X.K., Luo, Y., Qi, Y. and Zhang, R. (2010) 'On non-Newtonian lubrication with the upper convected Maxwell model', *Applied Mathematical Modelling*, 30(2010), pp. 1 – 15.

Marinca, V., Ene, R.D., Marinca, B. and Negrea, R. (2014) 'Different approximations to the solution of upper-convected Maxwell fluid over a stretching plate', *Hindawi Publishing Corporation, Abstract and Applied Analysis.* Article ID 139314, pp. 1-12.

Mukhopadhyay, S (2012) 'Upper-convected Maxwell fluid flow over an unsteady stretching surface embedded in porous medium subjected to suction/blowing', *Z. Naturforsch.* 67a, pp. 641-646.

Mukhopadhyay, S and Gorla, R.S.R. (2012) 'Unsteady MHD boundary layer flow of an upper convected Maxwell fluid past a stretching sheet with first order

constructive/Destructive chemical reaction', *Journal of Naval Architecture and marine Engineering*, pp. 123 – 133.

Peter, B.A., Ogunsola, A.W., Itodo, A.E., Idowu, S.A. and Mustapha, M.M. (2019a) 'A non-isothermal reacting MHD flow over a stretching sheet through a saturated porous medium', *American Journal of Mathematical and Computational Sciences.* 4(1), pp. 1-10.

Peter, B.A., Ogunsola, A.W., Itodo, A.E., Idowu, S.A. and Mustapha, M.M. (2019b) 'Reacting flow of temperature-dependent variable permeability through a porous medium in the presence of Arrhenius reaction', *American Journal of Mathematical and Computational Sciences,* 4(1), pp. 11-18.

Uscilowska, A. (2008) 'Non-Newtonian Fluid Flow in a Porous Medium', *Journal of Mechanics of Materials and Structures,* 3(6), pp. 1151-1159.

Vajravelu, K., Li, R., Dewasurendra, M., Benarroch, J., Ossi, N., *et al.* (2017) 'Analysis of MHD boundary layer flow of an upper-convected Maxwell fluid with homogeneous-heterogeneous chemical reactions', *Communications in Numerical Analysis,* 2017(2), pp. 202-216.

Vidyasagar G., Bala Anki Reddy P., Ramana B. and Sugunamma V. (2012) 'Mass transfer effects on radiative MHD flow over a non-isothermal stretching sheet embedded in a porous medium', *Pelagia Research Library*, 3(6), pp. 4016 – 4029.